

Synthesis and characterization of multiwalled carbon nanotube reinforced ultra high molecular weight polyethylene composite by electrostatic spraying technique

S.R. Bakshi, J.E. Tercero, A. Agarwal *

Department of Mechanical and Materials Engineering, Florida International University, Miami, FL 33174, United States

Received 6 February 2007; received in revised form 2 July 2007; accepted 1 August 2007

Abstract

In the present work, multiwalled carbon nanotube (MWNT) reinforced UHMWPE composite films were prepared by electrostatic spraying followed by consolidation. X-ray diffraction and differential scanning calorimetry studies showed a decrease in the crystallinity of UHMWPE due to the nature of the fabrication process as well as addition of MWNT. Tensile test showed an 82% increase in the Young's modulus, decrease in stress to failure from 14.3 to 12.4 MPa and strain to failure from 3.9% to 1.4% due to 5% addition of MWNT. Raman spectra showed the presence of compressive stresses in the nanotubes. Fracture surface showed presence of pullout like phenomena in the MWNT reinforced film.

© 2007 Elsevier Ltd. All rights reserved.

Keywords: A. UHMWPE; A. Multiwalled carbon nanotube; B. Stiffness; C. Mechanical testing

1. Introduction

Ultrahigh molecular weight polyethylene (UHMWPE) has been the choice of material for bio-implants, like artificial hip cups and tibial inserts, since it was first introduced in 1962 [1]. The properties required for such applications include high strength and stiffness, good fatigue and wear resistance, the necessary property being bio-compatibility. UHMWPE has also found application as a structural material in the form of fibers. UHMWPE fibers are commercially available under the trade names Dyneema and Spectra which claim to be up to 40% stronger than Aramid. Strength of the fibers have been specified as 2–4 GPa and they have been measured to be around 2 GPa [2]. They have been proposed for use in bulletproof vests, bow strings, climbing equipment, fishing line and high performance sails in yachting. Various techniques have been used to increase the strength and stiffness of UHMWPE. These

include cross-linking [3,4], self-reinforcement with UHMWPE fibers [2], reinforcement with carbon fibers [5], reinforcement with nanoparticles [6,7] and reinforcement with carbon nanotubes [8–12]. UHMWPE reinforced with carbon fibers have shown to be inferior in wear and fatigue resistance in body implants as compared to UHMWPE [5]. Recently Fang et al. have reported UHMWPE composites reinforced with hydroxyapatite nanoparticles, processed by combined swelling/twin-screw extrusion, compression molding and then seems extra hot drawing, having properties comparable to the cortical bone [7].

Since their discovery in 1991, carbon nanotubes have been used extensively as reinforcement for polymers. This has been reviewed in a number of publications [13–15]. Carbon nanotubes (CNTs) have been proposed for a number of applications due to their unique properties [16]. Polymer-CNT composite films have been prepared by many methods some of which include (i) sonicating a mixture of polymer dissolved in a solvent and carbon nanotubes followed by evaporation of solvent or drop casting

* Corresponding author.

E-mail address: agarwala@fiu.edu (A. Agarwal).

[17–19] (ii) processing of polymer-CNT mixture in molten state [20,21] and (iii) layer by layer assembly [22].

There are only a few literatures on CNT reinforced polyethylene. Tang et. al. [8] prepared composite films of High density polyethylene (HDPE)/MWNT composite containing up to 5 wt% MWNT by melt processing. They found an increase in the stiffness and work to failure of 7.88% and 4.95% respectively for the 5 wt% composite. Ruan et. al. [9] reported an increase in the ductility by addition of 1 wt% MWNT to UHMWPE films processed by solution casting. Wang et. al. [10] prepared UHMWPE fibers reinforced with MWNT by gel spinning. They reported very small increase in the tensile strength and modulus by addition of 3 wt% MWNT. Xue et al. [11] prepared UHMWPE–20 wt%HDPE and UHMWPE–HDPE–CNT blends by mixing the melt in a kneader and then hot pressing into plates. They reported moderate increase in the yield strength from 25 to 30 MPa and Young's modulus from 1187 to 1495 MPa for 2 wt% MWNT addition. Wear rate increased by addition of HDPE but reduced on addition of MWNT. Ruan et. al. [12] have also reported the fabrication of ultra strong fibers based on UHMWPE/MWNT which have properties close to commercially available fibers like Kevlar. In the present study, thick and flexible composite films of UHMWPE reinforced with multiwalled carbon nanotubes were prepared by a novel route and were studied for the improvement in mechanical properties.

2. Experimental

2.1. Materials and processing

The UHMWPE powder used was Mipelon™ supplied by Mitsui Chemical America, Inc., New York, USA. It was in the form of white powder of bulk specific gravity 400 kg/m³ (UHMWPE density = 940 kg/m³) and a particle size between 20 and 30 µm. Multiwalled carbon nanotubes of more than 94% purity and outer diameter between 40 and 70 nm and length up to few µm were obtained from

Nanostructured and Amorphous Materials Inc., NM, USA. The UHMWPE powder was mixed with 5 wt% of MWNT in a jar mill for 4 h so that the nanotubes were distributed evenly throughout the powder. Fig. 1 shows the SEM of UHMWPE and the UHMWPE–MWNT Powders. The powders were sprayed onto a teflon coated substrate using an electrostatic powder coating system (Craftsman Powder Coat System). Spraying with the electrostatic spray system leads to a uniform deposition of UHMWPE–MWNT powder with negligible overspray and loss of CNT. The Teflon substrate with the spray deposited layer was heated in an oven, at 180 °C for 30–40 min for consolidating the powder film into a film. The melting point of UHMWPE is around 136 °C but it is very viscous at this temperature and consolidation takes a long time if done at the melting point. So it was necessary to perform consolidation at slightly higher temperature of 180 °C. After the required time the substrate was taken out of the oven and was allowed to cool in air. The solidified film was easily stripped from the substrate. The films thus obtained were of the order of 0.2 mm thick.

2.2. Characterization of film

X-ray diffraction of the powder and coating was carried out to determine the crystallinity and any possible degradation of the coating due to the fabrication process. XRD was carried out using Cu K α ($\lambda = 1.542 \text{ \AA}$) radiation in a Siemens D-500 X-ray diffractometer operating at 40 kV and 20 mA. Differential Scanning Calorimetry was carried out on the UHMWPE powder as well as UHMWPE – MWNT coating, to study the crystallinity and melting behavior of UHMWPE and any oxidation or degradation after melting. A Du Pont DSC2910 was used for the purpose. The test samples were prepared by encapsulating around 1 mg of the sample between two aluminum pans. The samples were heated from 50 °C to 240 °C at a heating rate of 10 °C/min. Argon gas was passed through the cell at a rate of 30 ml/min during the test. Micro-Raman spectroscopy was carried out on the coatings to study any possible

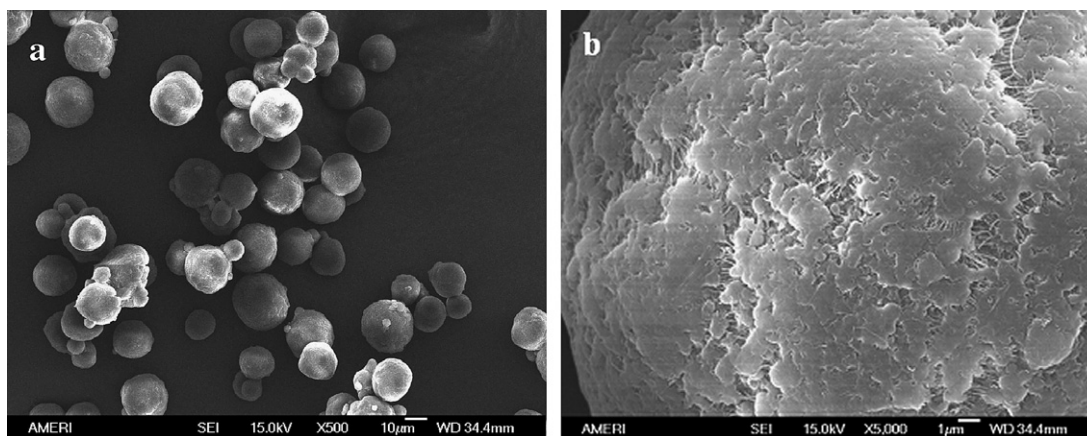


Fig. 1. SEM micrographs of (a) UHMWPE Powder and (b) UHMWPE–CNT powder mixture where CNTs are residing on UHMWPE surface.

degradation of the MWNT and/or the polymer as well as to analyze stresses and load transfer in the composite. Argon ion laser of wavelength 514.5 nm was used for this purpose and the Raman signal was measured in the back scattering mode. The laser power was 18 mW. A JEOL JSM-6330F field emission scanning electron microscope was used to study the fracture surfaces after the tensile test.

2.3. Tensile test

A standard punch was used to fabricate tensile samples from the thick films. The tensile tests were carried out on the samples using an EnduraTEC, ELF3200 series tensile tester with a maximum load of 18 N and maximum cross-head movement of 12 mm. The sample was in the shape of a dog bone with width of 2.75 mm. The gage length of the sample was 25 mm. The tests were carried out at a cross-head speed of 5 mm/min.

3. Results and discussion

3.1. XRD results

Fig. 2 shows the XRD patterns for the powders and the films. The peaks obtained correspond to the orthorhombic unit cell of polyethylene with lattice parameters $a = 7.41$ Å, $b = 4.96$ Å and $c = 2.54$ Å. It can be seen that ratio of the intensity of the (110) peak to the intensity of the (200) peak is larger in both coatings as compared to the starting powder. This leads to the conclusion that the (110) planes of the micelles or crystallites are oriented parallel to the surface during solidification. It is seen that there is no degradation of UHMWPE due to the process. The crystallinity of the powder and films was calculated by measuring the area under the UHMWPE peaks and the total peak area and taking the ratio of the two. It was seen that the crystallinity of the UHMWPE powder was 56% while that of the UHMWPE film was 55% and that of the UHMWPE–5 wt% CNT film was 43%. The decrease in crystallinity in

the coatings as compared with starting powder can be attributed to the relatively higher rate of cooling of the films after the consolidation process. MWNT have been reported to have very high thermal conductivity of around 3000 W/mK [23], whereas HDPE and Low density polyethylene (LDPE) have thermal conductivity of around 0.26 W/mK at room temperature [24]. It has been reported that the percolation threshold for electrical conductivity of UHMWPE–MWNT composites is as low as 0.0004–0.0007% by volume [25]. So the thermal conductivity of the composite is expected to be enhanced greatly. Hence the cooling rate experienced while the UHMWPE–MWNT film solidifies is expected to be larger than the pure UHMWPE film. Thus a decrease in crystallinity is expected in the film with MWNT.

3.2. DSC Results

Fig. 3 shows the DSC scans of the samples. The peak in the DSC curve corresponds to the melting of UHMWPE and the area enclosed by the peak is equal to the heat

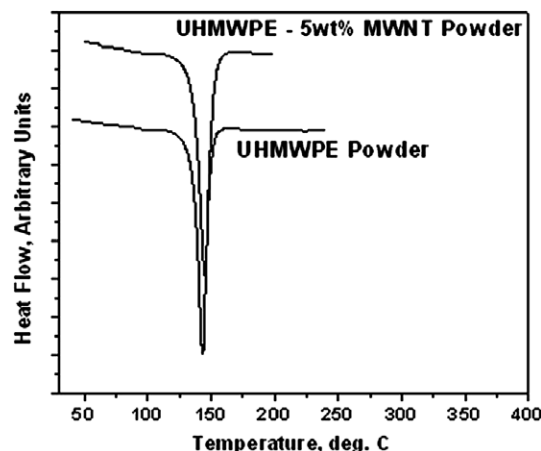


Fig. 3. DSC plots for the UHMWPE and UHMWPE–CNT powder mixture.

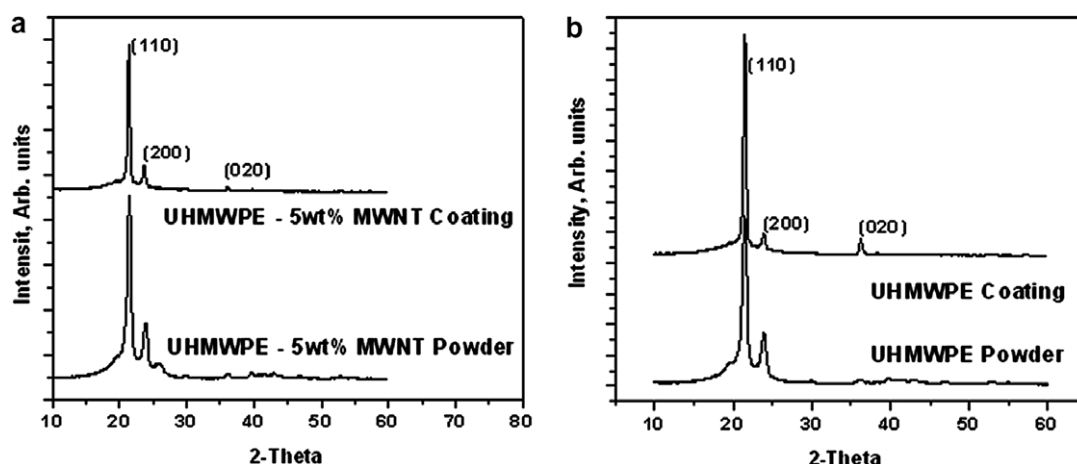


Fig. 2. XRD patterns of (a) UHMWPE powder and coating and (b) UHMWPE–CNT powder and coatings.

absorbed for melting. It is seen from the DSC plots that there is no indication of any kind of chemical reaction between MWNT and UHMWPE. For both the samples the melting temperature, calculated by the tangent method was 136 °C. The enthalpy of melting for the UHMWPE was 164.8 J/g while that for UHMWPE–MWNT was 132.7 J/g. The heat of fusion of 100% crystalline PE is 289.6 J/g [23]. The percentage crystallinity of UHMWPE, calculated on the basis of these values and the UHMWPE mass fraction, comes out to be 58% and 48%. The calculated values are close to those calculated from XRD plots. The addition of the MWNT reduces crystallinity. This is consistent with studies of McNally et al. [26] who prepared polyethylene MWNT composites by melt blending using a twin screw extruder. They reported a decrease in crystallinity in PE–MWNT composites from 32.5 to 27.6 for 10 wt% MWNT addition. One of the reasons for this is higher cooling rate experienced by the melt during solidification leading to lower time for arrangement of the chains to form crystallites. This has also been observed by Turrel and Belare [27] who have subjected UHMWPE melt at 170 °C to different crystallization conditions and found that isothermal crystallinity at 120 °C resulted in a crystallization of 52% while quenching in liquid nitrogen resulted in a crys-

tallinity of 34.6%. Other reason could be that nanotubes act as obstacles and hinder the mobility of the chains leading to lower amount of crystallization.

3.3. Micro-Raman spectroscopy results

Fig. 4a–c show the Raman spectra of the powders as well as the films. The peaks in Fig. 4a and b correspond to the standard peaks observed for UHMWPE. The Raman spectrum of UHMWPE has been reported earlier in literature and has been related to various aspects like crystallinity and deformation [9,28,29]. It has been reported that the position and full width at half-maximum (FWHM) of the Raman peak for C–C asymmetric stretching mode B_{1g} (1060 cm^{-1}) and the C–C symmetric stretching mode A_{1g} (1130 cm^{-1}) are sensitive to the strain present in sample [9,29]. It was reported [29] that there is a shift towards lower wave numbers for the above mentioned two peaks with small tensile strains (up to 1%) in the sample. A shift towards larger wave numbers is observed if the sample is subjected to compression. Also the FWHM increases, i.e. the peaks broaden, on application of tensile strains up to 3%. From Fig. 4b it is seen that there is small or no shift of the B_{1g} peak, which indicates that the matrix

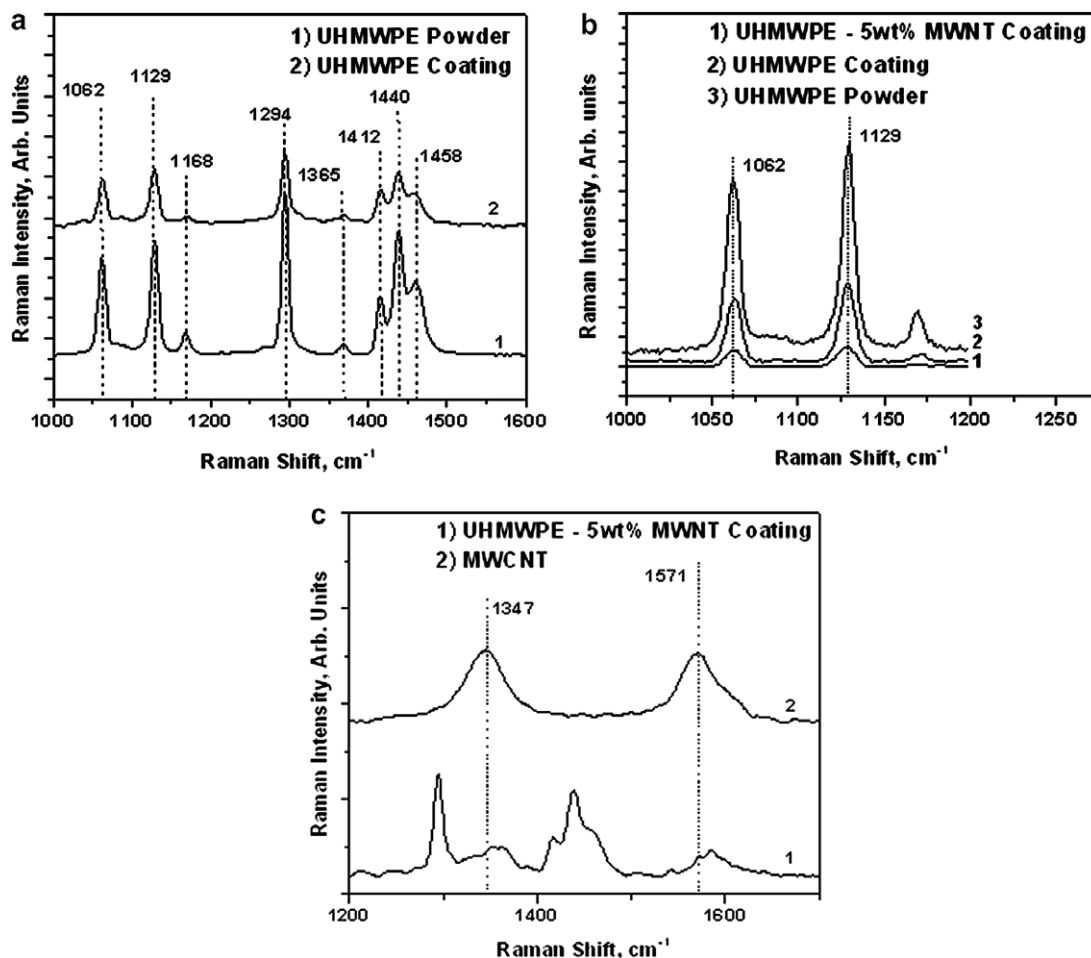


Fig. 4. Raman spectra plots (a) of UHMWPE powder and coating, (b) showing C–C stretching mode peaks and (c) showing peaks for MWCNT.

is stress free Fig. 4c shows the Raman peaks corresponding to multiwalled carbon nanotubes. The Raman spectrum of different types of carbon nanotubes and species has been well documented in literature [30]. For multiwalled carbon nanotubes, Raman peaks are generally observed at 1348 cm^{-1} (D – peak), 1574 cm^{-1} (G – peak) and at 2691 cm^{-1} (G' – peak). The G' – peak, which is the overtone of the D peak, has been observed to shift significantly when the nanotubes are stressed [31]. Similar to the UHMWPE, the G' peak shifts to lower wave numbers on application of tensile stress. It is seen from Fig. 4c that the D and G peak for MWNT shift towards larger wave numbers in the film, as compared to the MWNT sample, indicating compressive forces in the MWNT. Compressive stresses are attributed to the solidification shrinkage of the UHMWPE during the consolidation process. This suggests good intercalation of the polyethylene chains into the MWNT bundles and good load transfer between the matrix and the MWNT.

3.4. Tensile test results

Fig. 5 shows a picture of the tensile samples. The samples were prepared by punching the films with the punch. Fig. 6 shows the engineering stress strain curves for the

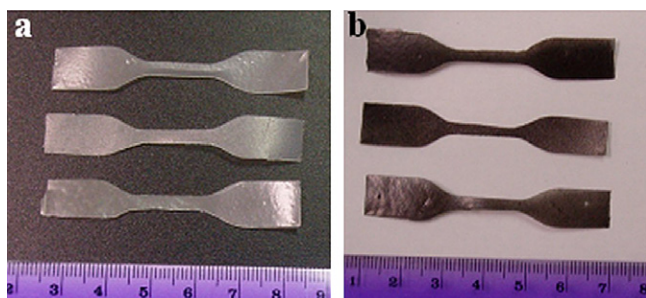


Fig. 5. Pictures of the tensile test samples of (a) UHMWPE and (b) UHMWPE–5 wt% MWNT.

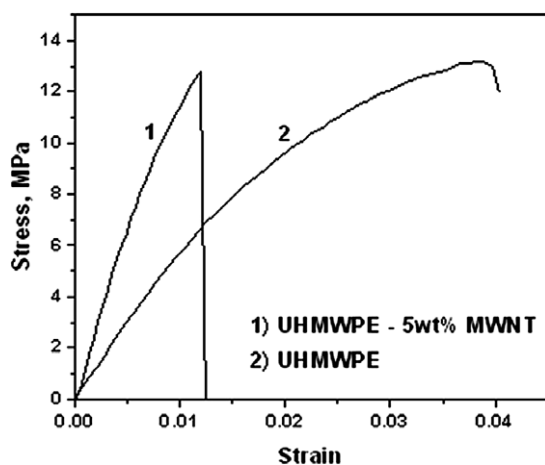


Fig. 6. Engineering stress strain curves for UHMWPE and UHMWPE–5 wt% MWCNT films.

UHMWPE and UHMWPE–5 wt% MWNT sample. The values presented here are an average of two tests. It can be seen that the strain to failure is more for the UHMWPE than the MWNT reinforced film. Also the Young's modulus of the MWNT reinforced film is larger than the UHMWPE film. The Young's modulus of UHMWPE and UHMWPE–MWNT film was found to be 682 MPa and 1240 MPa respectively. The maximum stress attained by the samples or the stress at fracture of UHMWPE and UHMWPE–MWNT film was found to be 14.3 MPa and 12.4 MPa respectively. The final strain at failure of UHMWPE and UHMWPE–MWNT film was found to be 3.9% and 1.4% respectively. It is seen that the stiffness of UHMWPE increases by 82% by incorporation of 5 wt% MWCNT but the strain to failure reduces drastically. The results are in contradiction to the ones obtained by Ruan et. al [9], where they have found that 1 wt% MWNT addition increases the toughness and ductility of the composite. As compared to their results, the Young's modulus of our UHMWPE is lower and they have reported even higher values for 1 wt% MWNT reinforced composite. There can be many reasons for this. Firstly, the thickness of their films was of the order of few tens of microns while those fabricated in this study were of the order of 0.2 mm. Also their films were hot drawn after solution casting while the films were not subjected to any post consolidation treatment in the present study. This might lead to a higher degree of defects like pores and improper or weak interfaces between UHMWPE particles in the present films. Improper consolidation may lead to premature failure and hence a low value of strain to failure. The decrease in the strain to failure could also be due to premature failure at MWNT clusters. Secondly, hot drawing might lead to better alignment, better dispersion and better matrix MWNT bonding which leads to better properties. Thirdly reason is that the fact that the MWNT used in this study are different than the ones used in their study and will have different properties. Fourthly, the UHMWPE powders used in previous study had a molecular weight of 6×10^6 g/mol while UHMWPE used in the present work has a molecular weight of 2×10^6 g/mol.

3.5. Fracture surface analysis

SEM was carried out to study the fracture surfaces of the films. Fig. 7 shows the fracture surfaces of the films. It can be seen that the fracture occurs in both cases by fibrous fracture. There is lot of plastic deformation in the UHMWPE matrix before fracture whereas the fracture occurs after small deformation in the MWNT reinforced film. Fig. 8 shows the high magnification SEM micrograph of the fracture surface of UHMWPE–5 wt% MWNT film. It can be seen that there are pullout like regions, marked by arrows, in Fig. 8a which are MWNT enveloped by a layer of polyethylene. It shows good wetting of MWNT by UHMWPE. This is very essential for efficient load transfer. As stated earlier, Raman spectroscopy showed the presence

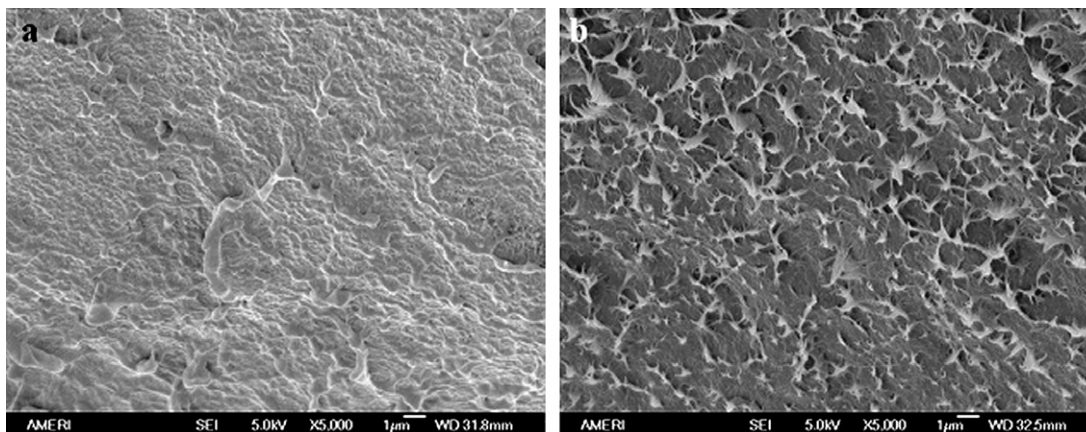


Fig. 7. SEM of fracture surface of (a) UHMWPE and (b) UHMWPE–5 wt% MWNT film.

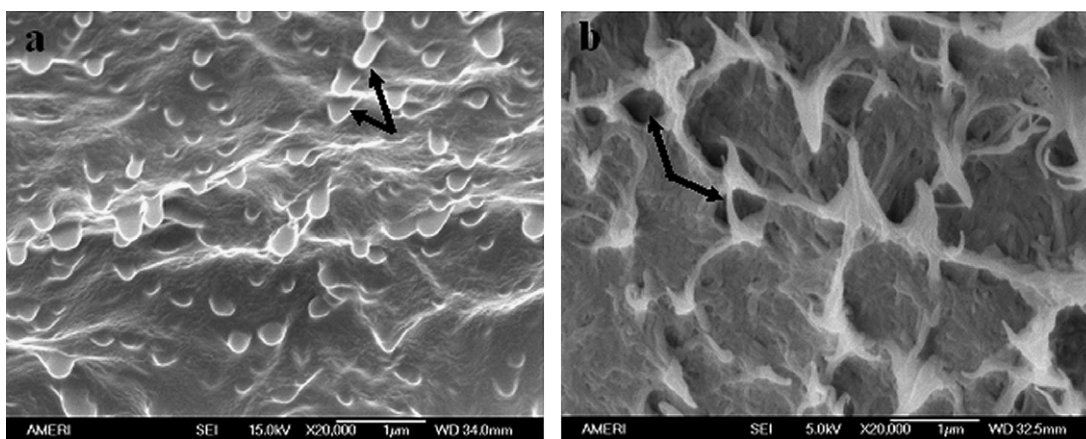


Fig. 8. High magnification SEM images of the fracture surface of UHMWPE–5 wt% MWCNT film showing (a) pull-out like phenomena and (b) regions from where pull-out occurred.

of compressive stresses in MWNT indicating good load transfer in the films. Fig. 8b shows cup like areas, marked by the arrows, from where the pullout has occurred. It can be seen that the failed fibrous UHMWPE matrix around the depression have undergone plastic deformation and then fracture. This indicates that the fibrils engulfed the MWNT and there is stress transfer between them. Failure by pullout suggests that it is due to the interfacial failure. Post consolidation treatments can increase the interfacial strength and improve the properties of the films.

4. Conclusions

1. Thick films of UHMWPE and UHMWPE–5 wt% MWCNT were successfully prepared by electrostatic spraying and consolidation by sintering/melting.
2. XRD shows a decrease in crystallinity of the MWNT reinforced film due to the faster cooling rates employed in the solidification of the coatings and the fact that the thermal conductivity of UHMWPE melt is enhanced by addition of MWNT. This could also be due to the fact the nanotubes decrease the mobility of the polymer chains.

3. Raman spectroscopy revealed presence of compressive stresses in MWNT. This is attributed to the stresses induced due to solidification shrinkage of UHMWPE. This again suggests good intercalation of polymer chains into MWNT clusters and load transfer between the two.
4. Tensile test shows 82% increase in Young's modulus due to addition of 5 wt% MWNT. But the addition of MWNT reduces the stress and strain to failure from 14.3 to 12.4 and 3.9% to 1.4% respectively, which is attributed to the premature failure at MWNT clusters.
5. SEM of fracture surface of UHMWPE–5 wt% MWCNT sample reveals pullout like phenomena and cup like depressions. This indicates that interface failure is the reason for the failure of the composite.

Acknowledgements

The authors would like to thank CeSMEC at FIU for carrying out Micro-Raman spectroscopy. The authors would like to thank Mr. Kantesh Balani for helping with the Raman spectroscopy and SEM characterization. The

authors would like to thank Dr. Rebecca Anderson from the Department of Biomedical Engineering at FIU for helping with the tensile test. One of the authors (S.R. Bakshi) would like to acknowledge Presidential Enhanced Assistantship from FIU for funding. Authors would like to acknowledge the research funding from the Office of Naval Research (N00014-05-1-0398) and NSF Career Award (NSF-DMI-0547178).

References

- [1] Li S. Ultra high molecular weight polyethylene: from Charnley to cross-linked. *Oper Techn Orthopaedics* 2001;11(4):288–95.
- [2] Deng M, Shalaby SW. Properties of self-reinforced ultra-high-molecular-weight polyethylene composites. *Biomaterials* 1997;18: 645–55.
- [3] Lewis G. Properties of crosslinked ultra-high-molecular-weight polyethylene. *Biomaterials* 2001;22:371–401.
- [4] Park K, Mishra S, Lewis G, Losby J, Fan Z, Park JB. Quasi-static and dynamic nanoindentation studies on highly crosslinked ultra-high-molecular-weight polyethylene. *Biomaterials* 2004;25:2427–36.
- [5] Wright TM et al. Failure of carbon fiber-reinforced polyethylene total knee-replacement components. A report of two cases. *J Bone Joint Surg Am* 1998;70:926–32.
- [6] Fang L, Leng Y, Gao P. Processing and mechanical properties of HA/UHMWPE nanocomposites. *Biomaterials* 2006;27:3701–7.
- [7] Fang L, Gao P, Leng Y. High strength and bioactive hydroxyapatite nano-particles reinforced ultrahigh molecular weight polyethylene. *Composites B* 2007;38:345–51.
- [8] Tang W, Santare MH, Advani SG. Melt processing and mechanical property characterization of multi-walled carbon nanotube/high density polyethylene (MWNT/HDPE) composite films. *Carbon* 2003;41:2779–85.
- [9] Ruan SL, Gao P, Yang XG, Yu TX. Toughening high performance ultrahigh molecular weight polyethylene using multiwalled carbon nanotubes. *Polymer* 2003;44:5643–54.
- [10] Wang Y, Cheng R, Liang L, Wang Y. Study on the preparation and characterization of ultra-high molecular weight polyethylene-carbon nanotubes composite fiber. *Compos Sci Technol* 2005;65:793–7.
- [11] Xue Y, Wu W, Jacobs O, Schadel B. Tribological behaviour of UHMWPE/HDPE blends reinforced with multi-wall carbon nanotubes. *Polym Test* 2005;25:221–9.
- [12] Ruan S, Gao P, Yu TX. Ultra-strong gel-spun UHMWPE fibers reinforced using multiwalled carbon nanotubes. *Polymer* 2006;47:1604–11.
- [13] Coleman JN, Khan U, Blau WJ, Gun'ko YK. Small but strong – a review of the mechanical properties of carbon nanotube-polymer composites. *Carbon* 2006;44:1624–52.
- [14] Tjong SC. Structural and mechanical properties of polymer nanocomposites. *Mater Sci Eng R* 2006;53:73–197.
- [15] Hussain F, Hojjati M, Okamoto M, Gorga RE. Polymer-matrix Nanocomposites, Processing, Manufacturing, and Application: An Overview. *J Compos Mat* 2006;40(17):1511–75.
- [16] Baughman RH, Zakhidov AA, de Heer WA. Carbon Nanotubes-the Route Towards Applications. *Science* 2002;297:787–92.
- [17] Schaffer MSP, Windle AH. Fabrication and Characterization of Carbon Nanotube-Polyvinyl alcohol Composites. *Adv Mater* 1999;11(11):937–41.
- [18] Jin L, Bower C, Zhou O. Alignment of carbon nanotubes in a polymer matrix by mechanical stretching. *Appl Phys Lett* 1998;73(9):1197–9.
- [19] Qian D, Dickey EC, Andrell R, Rantell T. Load transfer and deformation mechanisms in carbon nanotube-polystyrene composites. *Appl Phys Lett* 2000;76(20):2868–70.
- [20] Jin Z, Pramoda KP, Xu G, Goh SH. Dynamic mechanical behavior of melt-processed multi-walled carbon nanotube-polymethyl methacrylate composites. *Chem Phys Lett* 2001;337:43–7.
- [21] Zhang WD, Shen L, Phang IY, Liu T. Carbon Nanotubes Reinforced Nylon-6 Composite Prepared by Simple Melt-Compounding. *Macromolecules* 2004;37:256–9.
- [22] Olek M, Ostrander J, Jurga S, Mohwald H, Kotov N, Kempa K, Geisig M. Layer-by-Layer Assembled Composites from Multiwalled Carbon Nanotubes with Different Morphologies. *Nano Lett* 2004;4(10):1889–95.
- [23] Kim P, Shi L, Majumdar A, McEuen PL. Mesoscopic thermal transport and energy dissipation in carbon nanotubes. *Physica B* 2002;323:67–70.
- [24] Zhou W, Qi S, An Q, Zhao H, Liu N. Thermal conductivity of boron nitride reinforced composites. *Mater Res Bull* 2007. doi:10.1016/j.materresbull.2006.11.047.
- [25] Lisunova MO, Mamunya PY, Lebovka NI, Melezhyk AV. Percolation behavior of ultrahigh molecular weight polyethylene/multi-walled carbon nanotubes composites. *Eur Polym J* 2007. doi:10.1016/j.eurpolymj.2006.12.015.
- [26] McNally T et al. Polyethylene multiwalled carbon nanotube composites. *Polymer* 2005;46:8222–32.
- [27] Turrel Mary B, Bellare Anuj. A study of the nanostructure and tensile properties of ultra-high molecular weight polyethylene. *Biomaterials* 2004;25:3389–98.
- [28] Bertoluzza A, Fagnano C, Rossi M, Tinti A, Cacciari GL. Micro-Raman spectroscopy for the crystallinity characterization of UHMWPE hip cups run on joint simulators. *J Mol Struct* 2000;521:89–95.
- [29] Tarantili PA, Andreopoulos Galiotis C. Real-Time Micro-Raman Measurements on Stressed Polyethylene Fibers. 1. Strain Rate Effects and Molecular Stress Redistribution. *Macromolecules* 1998;31:6964–76.
- [30] Eklund PC, Holden JM, Jishi RA. Vibrational Modes of Carbon Nanotubes; Spectroscopy and Theory. *Carbon* 1995;33(7):959–72.
- [31] Cooper CA, Young RJ, Halsall M. Investigations into the deformation of carbon nanotubes and their composites through the use of Raman spectroscopy. *Compos Part A* 2001;32:4001–11.